Polarization-Mode Dispersion Measurements Along Installed Optical Fibers Using Gated Backscattered Light and a Polarimeter

Henrik Sunnerud, Bengt-Erik Olsson, Magnus Karlsson, Peter A. Andrekson, and Jonas Brentel

***Abstract*—We describe two new techniques that utilize a polarimeter for studying the state of polarization of gated Rayleigh-backscattered or Fresnel-backreflected light along optical fibers in real time on the Poincaré sphere. The first method, using Rayleigh-backscattered light, is here applied to measure the accumulation of polarization-mode dispersion (PMD) along an 11.5 km section of installed fiber link. With a simplified configuration, the second technique is developed and applied for measuring the PMD of individual fiber subsections in a 37 km long link. This is achieved by using the Fresnel-reflections which arise from the fiber connectors that join the link.**

***Index Terms*—Fresnel-reflections, installed fibers, Monte Carlo simulations, polarimeter, polarization-mode dispersion (PMD), Rayleigh-scattered light.**

I. Introduction

WHEN chromatic dispersion in optical fibers no longer limits the data-rate of transmission systems, polarization-mode dispersion (PMD) could become the major limiting factor. The tolerable amount of total average PMD depends on the bit-rate, and without PMD-compensation a value of approximately 10% of the bit-slot has been suggested [1]. Hence, for a 40-Gb/s channel bit-rate system, approximately 2.5-ps total average PMD can be accepted. However, for many installed links PMD is a severe limitation already at a bit-rate of 10 Gb/s while keeping the unrepeated link-length at 100 km and beyond. Installed links consist of individual subsections joint together at hubs, either by splices or by connectors. As the PMD can be varying among different parallel fibers within the same cable-section [2], a way to combat PMD of installed links would be to improve a few spans of the link by exchanging high-PMD fibers for fibers with low PMD within the same section, if available. Thereby, an upgrade of these spans to a higher transmission speed would be made possible and thus knowing the PMD of each individual subsection along the link would be sufficient. The hubs, where the fiber is accessible, would then constitute particular points of interest. Although various techniques exist for measuring the average PMD of a whole fiber, only a few measure the accumulation/distribution of PMD along a fiber-link [3]–[5]. These methods represent optical time-domain reflectometer (OTDR) techniques which measure the total backscattered signal. In this paper, we describe two techniques which aim at measuring the PMD-accumulation up to a few specific points of interest along an installed optical fiber. For this purpose we have developed a method that allows the application of a commercial polarimeter for studying the Rayleigh-backscattered or backreflected light, which is achieved by gating in the optical domain.

The first technique, which is described in Section II, makes use of the polarimeter for studying the polarization-state of the Rayleigh-scattered light (reflected at a specific position along the fiber) in real time on the Poincaré sphere. The method is here demonstrated by measuring the PMD-accumulation along an 11.5-km installed fiber-link. The technique works particularly well in the field, probably because of the longer polarization correlation length that we observed in the installed fiber as compared to spooled fiber in the laboratory.

At hubs along an installed link, fiber connectors often join sections together, giving rise to strong Fresnel-reflections when measuring backscattered light [2]. It would be very simple to change fibers and reroute the traffic at the hubs by switching connectors and thereby minimizing the PMD of some spans before the upgrade to a higher transmission speed. The second technique exploits these Fresnel-reflections, studying the backreflected light and measuring the PMD-accumulation up to each reflection-point along the link. As the backreflected power is usually much higher than the Rayleigh-backscattered power, a few important simplifications of the experimental set-up can be made, resulting in the second technique which is discussed in Section III. Fresnel-reflections have been used before in PMD measurements [6], but then limited to only one fiber span and under the condition that only one reflection is present. However, this is not always the case for installed optical fibers [2] and in reality, the input connector reflection is difficult to ignore. The optical gate which our techniques use, eliminates all these problems by selecting a proper temporal window in the backscattered/backreflected signal that is studied.

The main problem with all backscattering techniques is that they do not give all information about what happens in the forward direction of the fiber. Information is lost regarding circular birefringence [4] and the true differential group-delay (DGD) in

Manuscript received July 26, 1999; revised April 12, 2000. This work was supported by Chalmers Centre for High Speed Technology (CHACH) and the Swedish Research Council for Engineering Sciences.

H. Sunnerud, M. Karlsson, P. A. Andrekson, and J. Brentel are with the Photonics Laboratory, Department of Microelectronics, Chalmers University of Technology, SE-412 96 Göteborg, Sweden (e-mail: sunnerud@elm.chalmers.se).

B. E. Olsson was with the Photonics Laboratory, Department of Microelectronics, Chalmers University of Technology, SE-412 96 Göteborg, Sweden. He is now with the Department of Electrical and Computer Engineering, Optical Communication and Photonic Network Laboratory, University of California at Santa Barbara, Santa Barbara, CA 93106 USA.

Publisher Item Identifier S 0733-8724(00)05756-X.

the forward direction at any given wavelength cannot be directly obtained. However, we can determine the average DGD in the forward direction using measurements at several wavelengths.

The DGD in the forward direction is given by $\Delta\tau = |\,\boldsymbol{\Omega}| = \sqrt{\Omega_x^2+\Omega_y^2+\Omega_z^2}$ while the backscattered DGD is given by [4]: $\Delta\tau_B = |\boldsymbol{\Omega}_B| = 2\sqrt{\Omega_x^2+\Omega_y^2}$, where Ω_x, Ω_y and Ω_z are the components of the PMD-vector, $\boldsymbol{\Omega}$, in Stokes space. Hence, we can always measure a lower bound of the forward DGD at each specific wavelength, which is given by: $\Delta\tau \geq \Delta\tau_B/2$. To estimate the accumulated average DGD from the backscattered DGD, we use the relation [4]: $\langle\Delta\tau_B\rangle/\langle\Delta\tau\rangle = \pi/2$, which means that on average, we measure $\pi/2$ more DGD for the round-trip. However, $\langle\Delta\tau_B\rangle/(\pi/2)$ may differ from $\langle\Delta\tau\rangle$ due to the limited wavelength interval over which the average is taken. Also the average DGD, $\langle\Delta\tau\rangle$, measured over the wavelength interval $\Delta\lambda$, which is an estimation of the statistical average, $\langle\Delta\tau\rangle_\infty$, is affected by an error. In Section IV, the introduced error for the backscattering technique as function of DGD and wavelength interval is treated by means of Monte Carlo simulations.

II. Measurements of Rayleigh-Scattered Light

The measurement set-up is shown in Fig. 1. The pulse generator modulated a tunable external cavity laser (ECL), generating a short optical pulse which was amplified by an erbium-doped fiber amplifier (EDFA). An acoustooptical modulator (AOM) was used to suppress amplified spontaneous emission noise (ASE) generated in the EDFA and the high-power pulse was launched into the installed fiber cable. This pulse source, specially optimized for measurement of installed fiber, was also used in [2]. The Rayleigh-backscattered signal was subsequently amplified in an EDFA, followed by a second AOM. This AOM was used to select backscattered light from a specific position along the fiber and the state of polarization (SOP) was studied in real time with a polarimeter. If the SOP changes during the gate-time, then the polarimeter presents the average SOP and results in a lower degree of polarization (DOP). In this way, this polarimeter is quite robust to small SOP changes within the gate time. Also, by gating the signal in the optical domain, the detector bandwidth requirements are much lower, compared to techniques where the whole backscattered signal is studied simultaneously [2]–[4], [7]. All components after the polarizer were selected specifically for low PMD and low polarization-dependent loss (PDL) since they otherwise would contribute too much to the measured DGD. In our set-up the total DGD was $\langle\Delta\tau_0\rangle \approx 0.2$ ps, which was compensated for by a deconvolution of the measured average DGD, i.e., $\langle\Delta\tau_B\rangle \approx \sqrt{\langle\Delta\tau_{\rm tot}\rangle^2 - \langle\Delta\tau_0\rangle^2}$, where $\langle\Delta\tau_B\rangle$ is the backscattered average DGD of the fiber and $\langle\Delta\tau_{\rm tot}\rangle$ is the total average DGD.

The remaining nonpolarized ASE from the second EDFA is effectively omitted by the polarimeter even though the DOP decreases. The wavelength, λ, or the pulse-delay, $t = 2nL/c$, can now be changed and the SOP-evolution of the backscattered light can be studied in real time on the Poincaré sphere. The pulse repetition-frequency cannot exceed $f < c/(2nL_{\rm tot})$

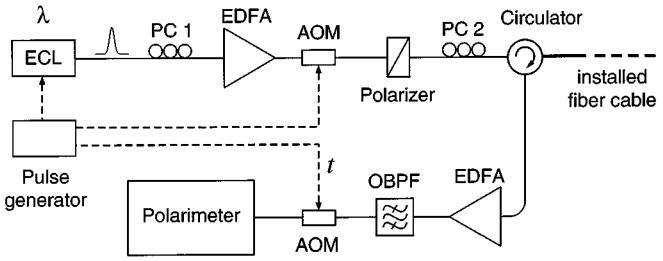

Fig. 1. Measurement setup. ECL: external cavity laser; PC: polarization-controller; AOM: acousto-optical modulator; EDFA: erbium-doped fiber amplifier; OBPF: optical bandpass filter.

to avoid interference between backscattered signals. Here, $L_{\rm tot}$ denotes the total length of the measured link, c the speed of light in vacuum and n the refractive index of the fiber.

To determine the DGD between the two principal SOP's of the backscattered light, we measure the change in SOP as a function of wavelength ($\delta\boldsymbol{s}/\delta\lambda$) for two different input polarizations. The PMD-vector can then be written as [8]

$$\boldsymbol{\Omega}_B = \frac{\dfrac{d\boldsymbol{s}_i}{d\omega}\times\dfrac{d\boldsymbol{s}_j}{d\omega}}{\dfrac{d\boldsymbol{s}_i}{d\omega}\cdot\boldsymbol{s}_j} \approx \frac{\lambda^2}{2\pi c}\,\frac{\delta\boldsymbol{s}_i\times\delta\boldsymbol{s}_j}{(\delta\boldsymbol{s}_i\cdot\boldsymbol{s}_j)\,\delta\lambda} \tag{1}$$

where $\boldsymbol{s}_{i,\,j}(\lambda_k)$ are the output SOP's (where the subscripts i and j denote different input polarizations) and $\delta\boldsymbol{s}_{i,\,j}(\lambda_k) = \boldsymbol{s}_{i,\,j}(\lambda_{k+1}) - \boldsymbol{s}_{i,\,j}(\lambda_k)$. The modulus of the PMD-vector is the value of the DGD ($\Delta\tau_B = |\boldsymbol{\Omega}_B|$) in units of seconds. In practice, a large error in the calculations can occur when the output polarization-state is near one of the principle states, so that the cross-product in Equ. (1) is small. Therefore, three different input polarization-states were used to minimize this error, where pairs of measurements had to satisfy certain criteria described in [8]. These criteria aims at removing inaccurate measurements, where the SOP's are close to the principle states. The PMD-vector was then calculated as the average of the vectors that satisfied the criteria.

The test-link was a 11.5 km section of field-installed dispersion-shifted fiber (DSF). The installed fiber showed qualitatively different characteristics compared to spooled fiber, with a longer polarization correlation length, which relieves the demands regarding pulse-duration and gate-duration of the second AOM. These durations should correspond to a physical length shorter than the polarization correlation length. These circumstances makes the proposed technique particularly suitable for measurement on installed fiber-links. The relatively long polarization correlation length was also verified by the Polarization-OTDR technique [2].

The pulse- and gate-durations were chosen so that a high DOP was obtained. Both durations were chosen to 100 ns which worked well and corresponded to a spatial resolution of around 20 m. We also noted that there was one SOP that was more probable to detect, namely, the input SOP, as was shown in [10]. At the positions along the link where we chose to measure, the DOP was still high (above 70% which was limited by ASE noise)

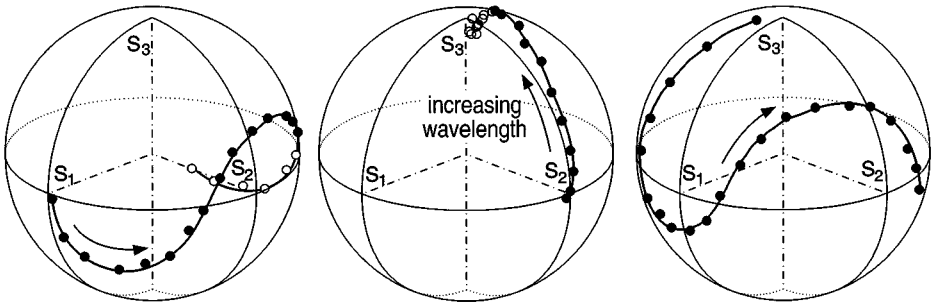

Fig. 2. Change in backscattered SOP's versus wavelength measured at 4 km over 10 nm in steps of 0.5 nm. Hollow symbols indicate back side of the Poincaré sphere. Initial output SOP's from left to right: s_1, s_2, s_3.

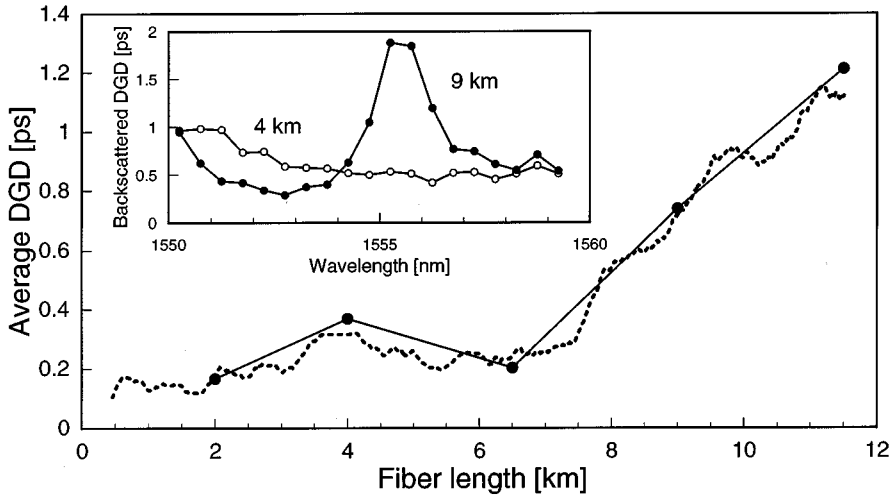

Fig. 3. Accumulated DGD versus fiber-length. New technique (•), distributed fixed-analyzer (dashed line). Inset: DGD versus wavelength for 4 km (○) and 9 km (•).

even if the detected SOP deviated from this most probable SOP, which shows that the spatial resolution was good enough.

Measurements of the DGD were performed at five different points along the fiber over a wavelength-range of 10 nm in steps of 0.5 nm. Fig. 2 shows how the backscattered SOP's, from a position 4 km into the fiber, change with wavelength for three different input polarization-states. Equation (1) was used to calculate the DGD-spectrum of the backscattered light from the five points along the fiber. The results are shown for 4 and 9 km in the inset of Fig. 3. Subsequently, the average DGD in the forward direction was estimated (compensated for the DGD in the components), which is shown in Fig. 3, for the five points. We can see that the PMD is very low in the first 7 km of fiber, while at 7 km, the PMD dramatically increases. The PMD in the first 7 km was estimated to 0.11 ps/$\sqrt{\text{km}}$ and to 0.55 ps/$\sqrt{\text{km}}$ in the last 4 km. The measurement was also compared with the distributed fixed-analyzer technique [3], [9] over 36 nm (dashed line in Fig. 3) with excellent agreement.

III. Fresnel-Reflection Measurements

The technique described above is best suited for measurements of a few points of interest along a fiber-link, in contrast to OTDR techniques, where many points along a fiber are measured simultaneously [2]–[4]. The next logical step is to take advantage from the Fresnel-reflections arising from fiber connectors, which often join an installed link together, with the result that a few important simplifications can be made. The situation is now much more favorable compared to measurements of Rayleigh-scattered light. The reflected fraction of power is higher than for the scattered light and the pulse-duration is no longer critical, as long as the reflections from different connectors do not interfere, which means that the pulse-duration can be increased to several microseconds. In this way, the average power-level into and out from the system can be substantially increased. As long as the incoming polarized average power to the polarimeter exceeds −70 dBm in our case, measurements can be performed with acceptable accuracy. The second EDFA, the optical filter, the polarizer and the polarization-controllers from the previous set-up can therefore be removed. Also, the input SOP can be controlled by the commercial polarimeter unit, which then can use the built-in Jones-matrix eigenanalysis method [11] for measuring the DGD of the backreflected light, making this technique practical and simple. The new configuration is shown in Fig. 4. If a reflection would be very weak, all average power will not originate from the reflection alone, but will partly consist of Rayleigh-scattered light. Fortunately, as the pulse is very

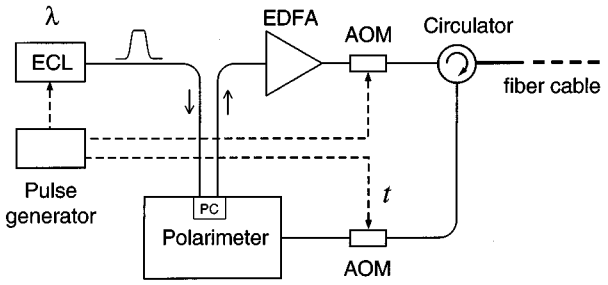

Fig. 4. Simplified set-up.

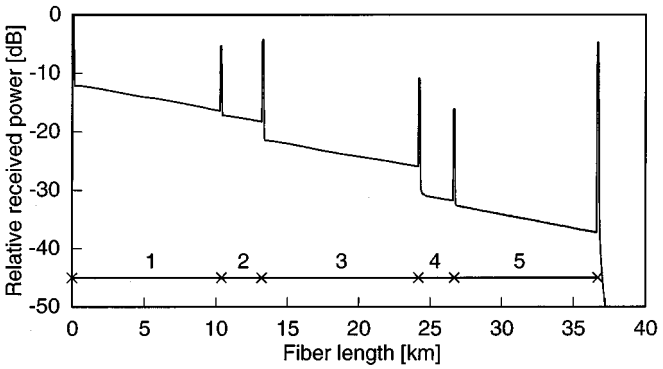

Fig. 5. Relative backscattered power from the characterized fiber-link consisting of five subsections. The reflection-coefficients were −38 dB in average.

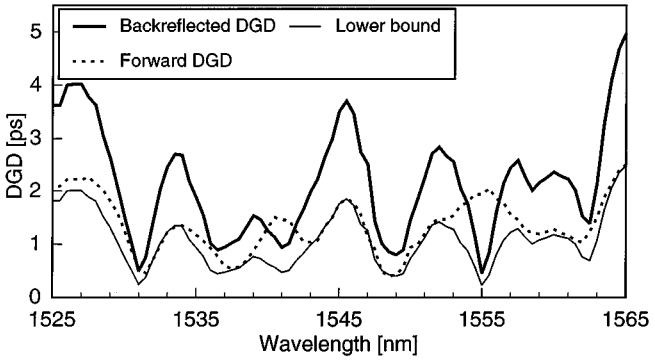

Fig. 6. Measured backreflected and forward DGD of the link at 37 km. The lower bound indicates $\Delta\tau_B/2$.

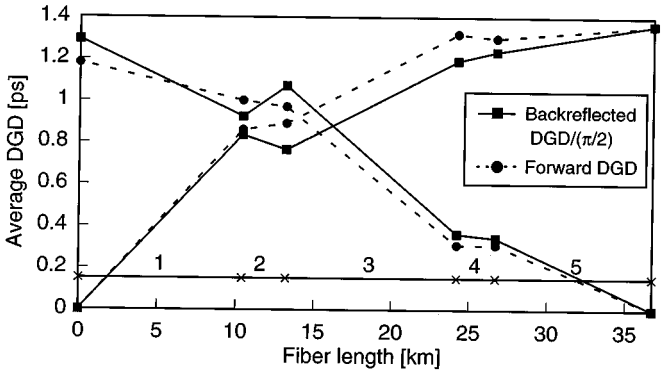

Fig. 7. Accumulated average DGD measured from both directions of the fiber-link. Wavelength-averaging interval $\Delta\lambda = 40$ nm.

long, most of the scattered power will be regarded as nonpolarized and effectively omitted by the polarimeter with the result that the DOP decreases. The condition that a majority of the received average power should originate from the reflection is fulfilled when the reflection-coefficient, ρ, is more than approximately −45 to −50 dB for pulse-durations below ∼1 μs. However, if the reflection is situated far from the input, so that the pulse suffers from high attenuation, then the reflection needs to be higher in order to reach an average power of more than −70 dBm to the polarimeter.

One application of this technique can be to measure the PMD of each individual subsection and identify high-PMD sections in order to exchange these for parallel fibers with lower PMD within the same cable. Thereby, some spans of the link could be improved before the upgrade to a higher transmission speed. Of course, some spans will also be degraded and cannot be upgraded.

An optical fiber-link was simulated by joining five individual sections by connectors, forming a 37-km long link. Fig. 5 shows the received power from the link relative to the input connector reflection-level with the Fresnel-reflections arising from the fiber connectors. The reflection-coefficients were −38 dB in average. The pulse-delay, $t = 2nL/c$, to the second AOM was adjusted so that a specific connector was selected for the measurement. The DGD-spectra of the backreflected light from the connectors in the link, $\Delta\tau_B(\lambda, L_i)$, as well as the forward DGD, $\Delta\tau(\lambda, L_i)$, up to the same fiber connectors (at L_i) were measured in both directions of the link and over a wavelength interval of 40 nm in steps of 0.5 nm. Fig. 6 shows an example of the obtained results. We compare $\Delta\tau_B$ with $\Delta\tau$ for $L = 37$ km. The backscattered DGD gives information about a lower bound of the true DGD ($\Delta\tau \geq \Delta\tau_B/2$) according to the discussion in Section I above. As can be seen from the figure, this bound holds. Note that the lower bound very often coincides with its maximum value. Why this occurs is explained in Section IV below. Subsequently, the average round-trip DGD, measured over the wavelength interval $\Delta\lambda$, was calculated and divided by $\pi/2$ to provide the estimate, $\langle\Delta\tau_B\rangle/(\pi/2)$, of the true average DGD, $\langle\Delta\tau\rangle_\infty$. The results from the measurements at all reflections and in both directions are shown in Fig. 7 (squares). They were compared with the accumulated conventionally measured DGD (filled circles) and a very good agreement was obtained in both directions. There is a discrepancy between these two entities because of the limited wavelength interval. In addition, the measured average DGD itself, $\langle\Delta\tau\rangle$, will be affected by an error and may deviate from the true average DGD. The total error can be decomposed into these two effects and is analyzed in Section IV.

From the measured backscattered DGD data, the PMD in ps/$\sqrt{\text{km}}$ of each subsection was roughly estimated, assuming a quadratic summation of the average DGD in each individual section. The obtained results are presented in Table I and shows the estimated PMD-coefficients measured in both directions, compared with the conventionally measured PMD-coefficients, which also were measured for each individual section. Note that these were measured over the same wavelength interval. The

TABLE I
ESTIMATED PMD-COEFFICIENTS COMPARED TO THE CONVENTIONALLY MEASURED COEFFICIENTS IN ps/$\sqrt{\text{km}}$

	PMD 1→5	PMD 1←5	Measured PMD
Fiber 1	0.26	0.25	0.27
Fiber 2	–	–	0.075
Fiber 3	0.27	0.30	0.32
Fiber 4	0.21	0.076	0.042
Fiber 5	0.18	0.11	0.10

first column shows the estimated PMD when the measurement was performed in the 1→5 direction, which means that the light was inserted at the fiber 1 end, etc. Generally, it is easier to obtain a good estimate of a section that is situated early in the link. The reason for this is that the average DGD grows approximately by the square-root of the fiber-length, i.e. the relative contribution to the increase of the total DGD is smaller for a fiber situated further away in a link. Still, a very good agreement is obtained for fiber 1, 3, and 5 (with the exception of fiber 5 in the 1→5 direction of measurement), which are all long and have high PMD. The accuracy is poor for fibers with low DGD. For fiber 2, the backreflected DGD decreases in both directions (see Fig. 7). The reason for this is that fiber 2's additional contribution to the total DGD is small compared to the uncertainty. Hence, it is impossible to find an estimate of the PMD for this fiber. However, this is not critical since this method aims at the identification of the high-PMD sections. Furthermore, this technique has great potential of measuring long links. We have been able to characterize a 129-km-long fiber-link using the end reflection. The link consisted of new-spooled, low-PMD standard single-mode fiber with an average DGD of 0.760 ps (i.e., PMD $= 0.07$ ps/$\sqrt{\text{km}}$). The round-trip DGD was measured to 1.14 ps over 40 nm and the ratio between the two is then 1.50, a discrepancy of 4.5% from the predicted value of $\pi/2$. Additionally, if a further enhancement of the dynamic range is needed, then another EDFA can be reintroduced.

IV. ERROR ESTIMATION

The DGD is a statistical quantity which varies over time and wavelength. Generally, wavelength-averaging is utilized to obtain an estimate, $\langle\Delta\tau\rangle$, of the true average DGD, $\langle\Delta\tau\rangle_\infty$. As this wavelength interval, $\Delta\lambda$, in practice is finite, there is an uncertainty in the estimation, which is an inherent limitation for all measurement principles and is also affecting the backscattering technique. By means of numerical simulations, we first investigated the introduced error, ϵ_1, for the estimation of the true average DGD from data measured in the forward direction. This was analyzed more thoroughly in [12]. Subsequently, we studied the corresponding error for the backscattering technique, ϵ_2. This error can be decomposed into two terms, of which one is the error ϵ_1, while the other is referred to as ϵ_3 and describes the discrepancy between the backscattered DGD, $\langle\Delta\tau_B\rangle$, and the conventionally measured DGD, $\langle\Delta\tau\rangle$, where both are measured over the same wavelength interval $\Delta\lambda$, under condition that the PMD-characteristics have not changed. This discrepancy is also of interest as it reflects the error experienced in the measurements over a finite wavelength interval.

The estimation of the true average DGD from data measured in the forward direction introduces an error which is given by

$$\epsilon_1 = \frac{\langle\Delta\tau\rangle_{\Delta\lambda} - \langle\Delta\tau\rangle_\infty}{\langle\Delta\tau\rangle_\infty}. \tag{2}$$

Here, $\langle\cdot\rangle_{\Delta\lambda}$ represents averaging over the wavelength interval $\Delta\lambda$ and $\langle\cdot\rangle_\infty$ represents the statistical average, which here was given by the analytical expression $\langle\Delta\tau\rangle_\infty = \sqrt{8N/3\pi}L_C/\Delta v_g$, where N is the number of birefringent segments, L_C is the length of each segment and Δv_g is the velocity difference between the two orthogonal modes. The fiber was modeled as a series of 1600 birefringent segments with randomly varying orientation axes. We have found that the probability density functions (pdf) of the relative error is a function of $\Delta\lambda\cdot\langle\Delta\tau\rangle$ only. In the case of $\Delta\lambda\to 0$, the pdf of ϵ_1 will have a shifted Maxwellian distribution, $f(\epsilon_1)$, with root-mean-square (rms) width

$$\sigma_1 = \sqrt{E\{\epsilon_1^2\}} = \sqrt{\int \epsilon^2 f(\epsilon_1)d\epsilon} = \sqrt{3\pi/8 - 1} \approx 0.422.$$

The wider wavelength-averaging interval, the more narrow, symmetric and Gaussian-like will the pdf be, which means that the rms-error decreases with increasing wavelength interval.

Subsequently, we investigated the relative error, ϵ_2, which is introduced when estimating the true average DGD, $\langle\Delta\tau\rangle_\infty$ with the backscattered DGD $\langle\Delta\tau_B\rangle_{\Delta\lambda}$, averaged over the wavelength interval $\Delta\lambda$. This error is given by

$$\epsilon_2 = \frac{\langle\Delta\tau_B\rangle_{\Delta\lambda}/(\pi/2) - \langle\Delta\tau\rangle_\infty}{\langle\Delta\tau\rangle_\infty}. \tag{3}$$

In the case of $\Delta\lambda\to 0$, the pdf of ϵ_2 will have a shifted Rayleigh distribution with rms-width $\sigma_2 = \sqrt{E\{\epsilon_2^2\}} = \sqrt{4/\pi - 1} \approx 0.523$, which means that the rms-error is 24% higher for the backscattering technique in this limit.

Finally, we studied the relative average discrepancy between the estimated average DGD obtained from the backscattering measurement and the average DGD measured in the forward direction. It is given by

$$\epsilon_3 = \frac{\langle\Delta\tau_B\rangle/(\pi/2) - \langle\Delta\tau\rangle}{\langle\Delta\tau\rangle} \tag{4}$$

and has zero mean in the strong mode-coupling regime. Here, $\langle\cdot\rangle$ represents averaging over the wavelength interval $\Delta\lambda$. In contrast to the other errors, this has a higher bound ($\epsilon_3 \le 4/\pi - 1$).

In Fig. 8, we show the pdf, $f(\epsilon_3, \Delta\lambda)$, for four cases; no averaging ($\Delta\lambda\to 0$) and $\Delta\lambda = 10$, 40 and 80 nm at an average DGD of 1.0 ps. For a very narrow wavelength interval ($\Delta\lambda\to 0$), the pdf is very sharp at $\epsilon_3 = 4/\pi - 1 \approx 0.27$, which means that the backscattered DGD has a high probability to reach its maximum value. Consequently, this enhances the relevance of the lower bound of the true DGD discussed above. In this limit, the pdf coincides with the analytical expression for the pdf (see Appendix)

$$f(\epsilon_3) = \frac{\pi}{4}\frac{y}{\sqrt{1-y^2}}, \qquad y \in [0, 1] \tag{5}$$

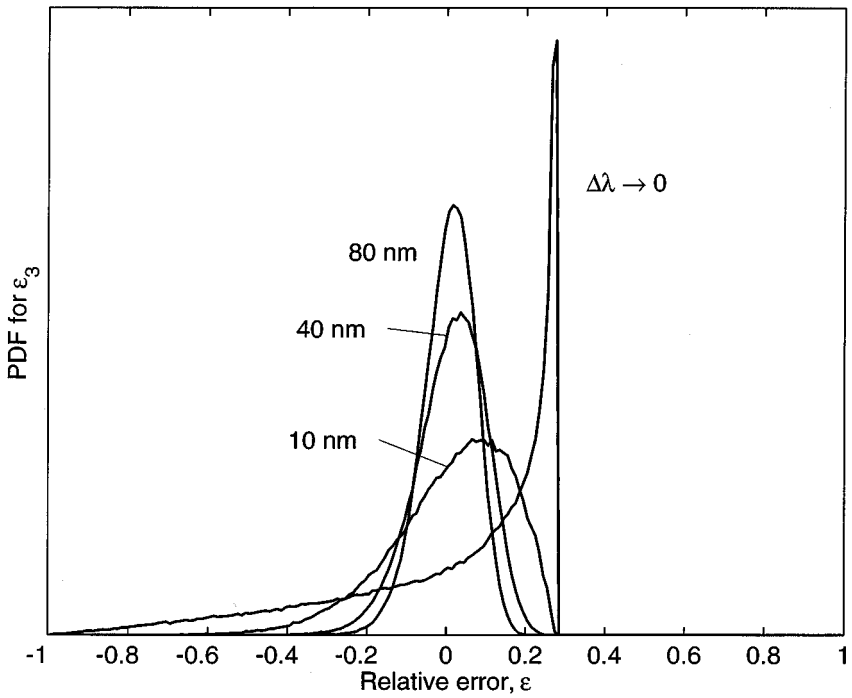

Fig. 8. Probability density functions for the error introduced due to the uncertainty of the backscattered DGD compared to the DGD measured in the forward direction for four different cases: no wavelength-averaging ($\Delta\lambda \to 0$) and wavelength-averaging intervals $\Delta\lambda = 10,\ 40$ and 80 nm. The average DGD is 1.0 ps.

where $y = \pi(1+\epsilon_3)/4$. The rms-discrepancy is

$$\sigma_3 = \sqrt{\int \epsilon^2 f(\epsilon_3) d\epsilon} = \sqrt{32/3\pi^2 - 1} \approx 0.284.$$

By contrast, the wider averaging wavelength interval, the more symmetric and Gaussian-like is the pdf.

The error for the backscattering technique can also be expressed as $\epsilon_2 = \epsilon_1 + \epsilon_3 + \epsilon_1\epsilon_3$. The mean value $E\{\epsilon_2\} = 0$, which shows that the mean value $E\{\epsilon_1\epsilon_3\} = 0$ since $E\{\epsilon_1\} = E\{\epsilon_2\} = 0$.

Fig. 9 shows the different rms-errors, $\sigma_i = \sqrt{E\{\epsilon_i^2\}} = \sqrt{\int \epsilon^2 f(\epsilon_i,\ \Delta\lambda\langle\Delta\tau\rangle)\, d\epsilon}$, i.e., the standard deviation of the error distributions, as function of wavelength-averaging interval and average DGD. In the limit $\Delta\lambda\langle\Delta\tau\rangle \to 0$, the simulated rms-errors agree very well with the analytical values.The rms-errors decreases with increasing average DGD and with increasing wavelength interval, as expected. If we assume that ϵ_1 is statistically independent of ϵ_3, the variance of ϵ_2 can be calculated as $\sigma_2^2 = E\{\epsilon_2^2\} = \sigma_1^2 + \sigma_3^2 + \sigma_1^2\sigma_3^2$. In Fig. 9, the dashed line shows the validity of this formula. Furthermore, it is exact in the limit $\Delta\lambda \to 0$.

The rms-error σ_3 reflects the discrepancy we see in the measurements presented in Figs. 3 and 7. Note that this error is reduced in [2] and [3] by averaging also in the fiber-length-direction. The rms-error σ_2 shows the uncertainty of the backscattering techniques compared to the statistical average. All errors decreases approximately as $\sim 1/\sqrt{\langle\Delta\tau\rangle\Delta\omega}$ as suggested in [12], where $|\Delta\omega| = 2\pi c\Delta\lambda/\lambda^2$. The rms-error for the backscattering technique, σ_2, is approximately 10% higher than the customary error σ_1. Even if the relative errors decreases with increasing average DGD, the absolute errors, $\sigma_i \cdot \langle\Delta\tau\rangle$, increases. Together with the fact that the relative DGD-accumulation of a section is smaller when situated at the far end of a characterized link, this makes the PMD estimation less successful far from the input. In other words, if the accumulated DGD of one section is smaller than the error, then a poor accuracy is obtained for the PMD estimation, which is the case for fibers 2 and 4 in Section III. However, the error is small enough to fulfill our purposes; to identify high-PMD fiber sections.

V. Discussion and Conclusions

We have described two closely related techniques which allow the utilization of a commercial polarimeter for studying the SOP of Rayleigh-backscattered or backreflected light along optical fibers in real time on the Poincaré sphere. This was achieved by optical gating. Both techniques are particularly useful for measurement of installed fiber-links. We have successfully measured the DGD-spectra of the Rayleigh-scattered signal along an installed fiber-link, which gives a lower bound of the true DGD at each specific wavelength. By averaging over the whole spectral range, we have also estimated the average DGD accumulation. The result was compared with the distributed fixed-analyzer technique, with excellent agreement.

By benefitting from the Fresnel-reflections arising from fiber connectors which join a link together, some significant simplifications in the set-up could be made. The PMD-coefficients of each individual subsection of a 37-km-long link were estimated and a very good agreement was found with the true PMD-coefficients for the high-DGD sections. The technique is relatively simple and has great potential of measuring long links.

Finally, the introduced error related to the uncertainty of the average DGD of the backscattered light compared to the real

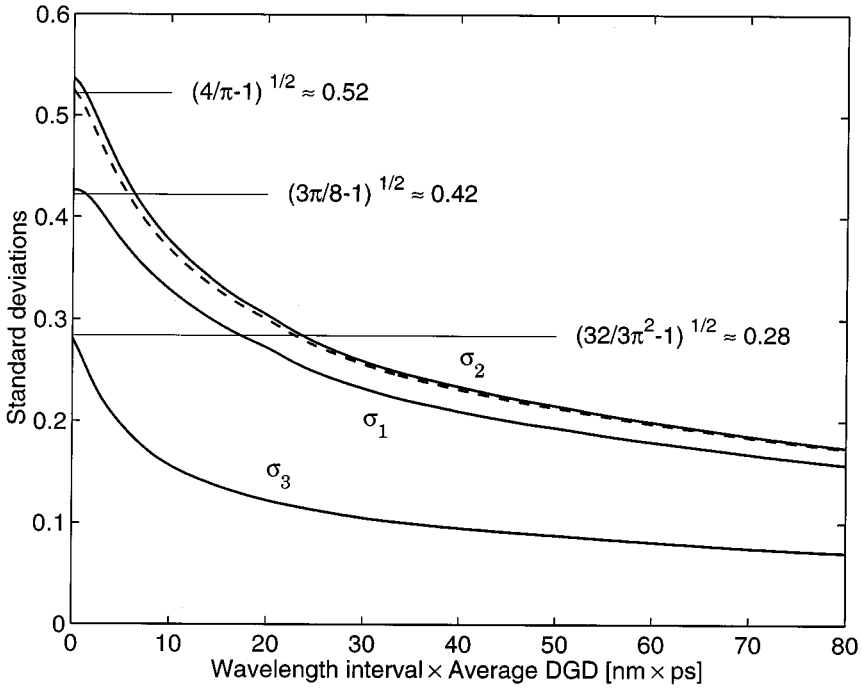

Fig. 9. The rms-widths, σ_i, of the error distributions as function of wavelength interval times the average DGD. Dashed line (- -): $\sigma_2 = \sqrt{\sigma_1^2 + \sigma_3^2 + \sigma_1^2\sigma_3^2}$.

average DGD (both averaged over the interval $\Delta\lambda$ and the statistical mean) was estimated by means of Monte Carlo simulations. The rms-error decreases with increasing average DGD and with increasing wavelength-averaging interval, as expected.

A comparison between the described techniques and the distributed fixed-analyzer technique [3] would be similar to a comparison between the classical Poincaré sphere- [8] and the Jones matrix-methods [11] on one hand and the well known fixed-analyzer technique [13] on the other. The wavelengths-resolved techniques are better for measurement of low-PMD links with a higher accuracy which can be obtained in a smaller spectral range. The described technique also has the potential for estimation of the true DGD-spectrum, which is subject to further investigations.

APPENDIX
CALCULATION OF pdf

Polarization-mode dispersion in an optical fiber is characterized by the PMD-vector $\mathbf{\Omega}$. The DGD is the modulus of the PMD-vector, i.e.

$$\Delta\tau = |\mathbf{\Omega}| = \sqrt{\Omega_x^2 + \Omega_y^2 + \Omega_z^2} \tag{6}$$

while the backscattered DGD is given by [4]

$$\Delta\tau_B = |\mathbf{\Omega}_B| = 2\sqrt{\Omega_x^2 + \Omega_y^2} \tag{7}$$

which means that one of the components of the PMD-vector cannot be measured. Consider the ratio between the backscattered- and the conventionally measured DGD, $X = \Delta\tau_B/\Delta\tau$, which is regarded as a stationary stochastic process. Depending on the direction of the random vector, $\mathbf{\Omega}$, this ratio may vary between 0 and 2. For the purpose of calculating the probability density function (pdf) of this ratio, we take the following step:

$$X = \frac{\Delta\tau_B}{\Delta\tau} = \frac{2\sqrt{\Omega_x^2 + \Omega_y^2}}{\sqrt{\Omega_x^2 + \Omega_y^2 + \Omega_z^2}} = 2|\sin\xi|$$
$$= 2\sqrt{1 - \cos^2\xi}, \qquad \xi \in [0, \pi], \tag{8}$$

where ξ is the random angle between the s_3-axis and $\mathbf{\Omega}$. Moreover, if $\cos\xi$ is uniformly distributed between -1 and 1, then this corresponds to a uniform distribution of $\mathbf{\Omega}$ on the Poincaré sphere. The probability function for X is then given by

$$F_X(x) = P(X \le x) = \int f_X(x')\,dx' = 1 - \sqrt{1 - (x/2)^2} \tag{9}$$

and finally, the pdf is equal to

$$f_X(x) = F_X'(x) = \frac{x/2}{2\sqrt{1 - (x/2)^2}}, \qquad x \in [0, 2]. \tag{10}$$

The expectation value of X is then $E\{X\} = \int x f_X(x)\,dx = \pi/2$, which also was calculated in [4], but in another way. An alternative derivation of the pdf for a function $\sin\xi$ is found in [13].

The relative discrepancy between the DGD estimation from a backscattering measurement and the forward DGD is given by

$$\epsilon = \frac{\Delta\tau_B/(\pi/2) - \Delta\tau}{\Delta\tau} = \frac{X}{\pi/2} - 1 \tag{11}$$

which has zero mean in the strong mode-coupling regime. The pdf for this relative error is given by

$$f(\epsilon) = \frac{\pi}{4}\,\frac{y}{\sqrt{1 - y^2}}, \qquad y \in [0, 1] \tag{12}$$

where $y = \pi(1+\epsilon)/4$ and $\epsilon \in [-1, 4/\pi - 1]$. The standard deviation of the relative error is

$$\sigma = \sqrt{\int \epsilon^2 f(\epsilon) d\epsilon} = \sqrt{32/3\pi^2 - 1} \approx 0.284.$$

ACKNOWLEDGMENT

The authors would like to thank J. Hansryd and also the reviewers for helpful suggestions.

REFERENCES

[1] H. Bülow, "Limitations of optical first-order PMD compensation," in *Proc. OFC'99*, San Diego, USA, Feb. 1999, Paper WE1.
[2] H. Sunnerud, B. E. Olsson, and P. A. Andrekson, "Measurement of polarization mode dispersion accumulation along installed optical fibers," *IEEE Photon. Technol. Lett.*, vol. 11, pp. 860–862, July 1999.
[3] ——, "Technique for characterization of polarization mode dispersion accumulation along optical fibers," *Electron. Lett.*, vol. 34, pp. 397–398, Feb. 19, 1998.
[4] F. Corsi, A. Galtarossa, and L. Palmieri, "Polarization mode dispersion characterization of single-mode optical fiber using backscattering technique," *J. Lightwave Technol.*, vol. 16, pp. 1832–1843, Oct. 1998.
[5] B. Huttner, B. Gisin, and N. Gisin, "Distributed PMD measurement with a polarization-OTDR in optical fibers," *J. Lightwave Technol.*, vol. 17, pp. 1843–1848, Oct. 1999.
[6] F. Corsi, A. Galtarossa, L. Palmieri, M. Schiano, and T. Tambosso, "Continuous-wave backreflection measurement of polarization mode dispersion," *IEEE Photon. Technol. Lett.*, vol. 11, pp. 451–453, Apr. 1999.
[7] J. G. Ellison and A. S. Siddiqui, "A fully polarimetric optical time-domain reflectometer," *IEEE Photon. Technol. Lett.*, vol. 10, pp. 246–248, Feb. 1998.
[8] C. D. Poole, N. S. Bergano, R. E. Wagner, and H. J. Schulte, "Polarization dispersion and principal states in a 147-km undersea lightwave cable," *J. Lightwave Technol.*, vol. 6, pp. 1185–1190, July 1988.
[9] H. Sunnerud, B. E. Olsson, M. Karlsson, and P. A. Andrekson, "Techniques for measurement of polarization mode dispersion accumulation along installed optical fibers," in *Proc. ECOC'99*, Nice, France, Sep. 1999, Paper II-6.
[10] M. O. van Deventer, "Polarization properties of Rayleigh backscattering in single-mode fibers," *J. Lightwave Technol.*, vol. 11, pp. 1895–1899, Dec. 1993.
[11] B. L. Heffner, "Automated measurement of polarization mode dispersion using Jones matrix eigenanalysis," *IEEE Photon. Technol. Lett.*, vol. 4, pp. 1066–1068, Sep. 1992.
[12] N. Gisin, B. Gisin, J. P. von der Weid, and R. Passy, "How accurately can one measure a statistical quantity like polarization-mode dispersion?," *IEEE Photon. Technol. Lett.*, vol. 8, pp. 1671–1673, Dec. 1996.
[13] C. D. Poole and D. L. Favin, "Polarization-mode dispersion measurements based on transmission spectra through a polarizer," *J. Lightwave Technol.*, vol. 12, pp. 917–929, June 1994.

Henrik Sunnerud, photograph and biography not available at the time of publication.

Bengt-Erik Olsson, photograph and biography not available at the time of publication.

Magnus Karlsson, photograph and biography not available at the time of publication.

Peter A. Andrekson, photograph and biography not available at the time of publication.

Jonas Brentel, photograph and biography not available at the time of publication.